Numerical Simulations for Dynamic WBAN Propagation Channel during Various Human Movements

Takahiro Aoyagi, Minseok Kim, Jun-ichi Takada
Tokyo Institute of Technology,
2–12–1, O-okayama, Meguro-ku, 152–8552, Japan
Telephone: +81–3–5734–2992
Email: aoyagi@ieee.org

Kiyoshi Hamaguchi, and Ryuji Kohno
Medical ICT Institute,
National Institute of Information and Communications Technology
3–4, Hikarino-oka, Yokosuka, 239–0847, Japan
Telephone: +81–46–847–5050
Fax: +81–46–847–5431
Email: hamaguti@nict.go.jp

***Abstract*— In this report, we performed six human movement simulation by a commercial software (Poser7). We performed FDTD simulations for body area network propagation with one transmitter and six receivers. Received amplitudes were calculated for every time frame of 1/30 s interval. We also demonstrated a polarization diversity effectiveness for dynamic wearable body area network propagation.**

I. Introduction

Recently, body area networks (BAN) make great attention in wireless communications. Both wearable BANs and implantable BANs are being discussed in the IEEE 802.15.6 standardization. To design a wireless communication systems, an electromagnetic propagation channel model is needed [1]. Several research groups, including our group, have developed implantable and wearable body area network channel models [2], [3], [4], [5], [6], [7], [8], [9], [10], [11], [12]. However, to make BAN channel models useful in actual situations, both intentional and unintentional human movements should be taken into account. Some experimental study have been performed for dynamic BAN channels [13], [14], [15], [16], [17], [18]. However, experiments for dynamic channel measurements of human movement have several difficulties and takes a lot of time. Thus construction of channel models for BAN propagation by electromagnetic field simulations is rather good idea. The on-body communication channels at 2.45 GHz have analyze by using an animation software for walking motion with 2.46 GHz [19] and 400 MHz [20]. In the ref. [20], the authors performed several human movement simulation for constructing a BAN channel model by using a commercial software. However, the electromagnetic wave propagation simulation was performed only for walking. In this report, we performed electromagnetic propagation simulation for six human movements by FDTD. From simulation results, we performed basic polarization diversity simulations for every movements. The results showed effectiveness of polarization diversity in wearable BAN.

II. Modeling human movements

We considered six human movements for dynamic body area networks channel analysis. These are walking (1s), sit/standing (2s), running (1s), sleeping (4s), changing-cloth (6.5s), and weak-walking(1s). Figure 1 shows the human movements. A commercial software for human posing (Poser 7, Smith Micro Software, Inc.) was used to make these poses. All movements were animated with 1/30s time resolution.

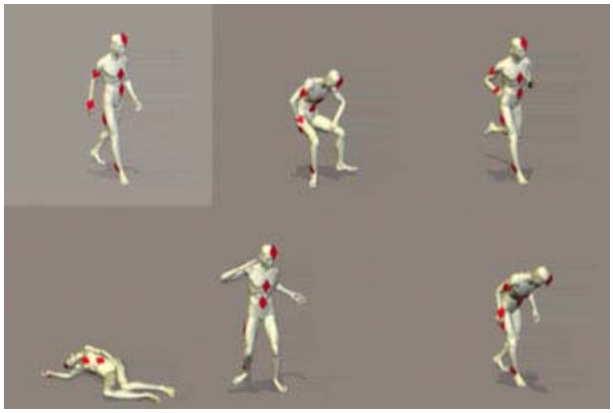

Fig. 1. Human movements analyzed in this report (Walking, Sit/standing, Running, Sleeping, Changing cloth, and Weak walking).

Figure 2 shows a diamond shaped marker for indicating antenna positions on the body surface. Directions parallel to longer diagonal of each marker are shown by vector $\mathbf{u}$, and directions parallel to the shorter diagonal of each marker are shown by vector $\mathbf{v}$. A transmitter was set at the navel of the body surface. Six receivers were set at head, right arm, right hand, chest, right thigh, and right ankle. All markers were set at 1.5cm above the body surface. The vector $\mathbf{u}$ and vector $\mathbf{v}$ of the markers were parallel to the body surface.

III. Numerical simulations

We performed electromagnetic wave propagation simulations for every movements by using FDTD. Calculated fre-

978-1-4244-9445-3/11/$26.00 ©2011 IEEE

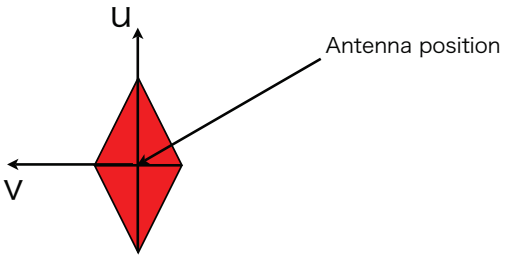

Fig. 2. Diamond shaped antenna position and direction marker

quency is 403.5 MHz, the center frequency of the MICS band. We extracted voxels from calculated human body poses for each animation frame. Figure 3 shows the example of the voxel for walking. Size of voxels is 5mm×5mm×5mm. Calculation area is 144×438×232 voxels for the first frame, for instance. Electric constants of the human body is assumed to these of averaged muscle [21], [22]. For 403.5 MHz, relative permittivity is 57.9 and conductivity is 0.82 (S/m). The calculation area is terminated by ten layers perfect matching layer. Sinusoidal wave is inputted into 5mm-length line electric current of $1\,\mathrm{A/m^2}$ at transmitter marker position. We calculated three directions (x, y, and z) of line source element located at the transmitter. The received electric field amplitudes were recorded at six receiver marker positions for three directions (x, y, and z). Thus 30×3=90 simulations have performed for one second. We used vector synthesis to calculate cases that the transmitter and the receivers are parallel to vector $\mathbf{u}$ or vector $\mathbf{v}$ of diamond shaped marker. We assume that u_x^0, u_y^0, and u_z^0 are components of the directional vector $\mathbf{u}^0$ of the transmitter; u_x^n, u_y^n, and u_z^n are components of the directional vector $\mathbf{u}^n$ of the n-th receiver; s_{pq}^{n0} are transfer coefficients of q-direction transmitter to p-direction n-th receiver where $p, q \in \{x, y, z\}$. The received level $R_{\mathbf{u}^n\mathbf{u}^0}$ of $\mathbf{u}^0$-direction transmitter to $\mathbf{u}^n$-direction n-th receiver is calculated as follows.

$$R_{\mathbf{u}^n\mathbf{u}^0} = \begin{pmatrix} u_x^n \\ u_y^n \\ u_z^n \end{pmatrix}^T \begin{pmatrix} s_{xx}^{n0} & s_{xy}^{n0} & s_{xz}^{n0} \\ s_{yx}^{n0} & s_{yy}^{n0} & s_{yz}^{n0} \\ s_{zx}^{n0} & s_{zy}^{n0} & s_{zz}^{n0} \end{pmatrix} \begin{pmatrix} u_x^0 \\ u_y^0 \\ u_z^0 \end{pmatrix} \quad (1)$$

Figure 4 to Fig. 12 show the temporal relative receive level of individual movements. Notations Tx$\mathbf{u}$-Rx$\mathbf{u}$ indicates that the direction of the transmitter is parallel to vector $\mathbf{u}$ and the direction of the receiver is parallel to vector $\mathbf{u}$. Other notations are similar, too. In the figures from Fig. 4 to Fig. 7, four combinations of Tx-Rx are shown. In the figures from Fig. 8 to Fig. 12, only combination of Tx$\mathbf{u}$-Rx$\mathbf{u}$ are shown.

IV. Polarization diversity effectiveness for wearable body area networks

According to the results above, it seems that polarization diversity has effectiveness for wearable body area network propagation. To show this, we performed simple statistical calculation and tested a basic polarization diversity algorithm. First, we considered the walking motion only. Figure I shows

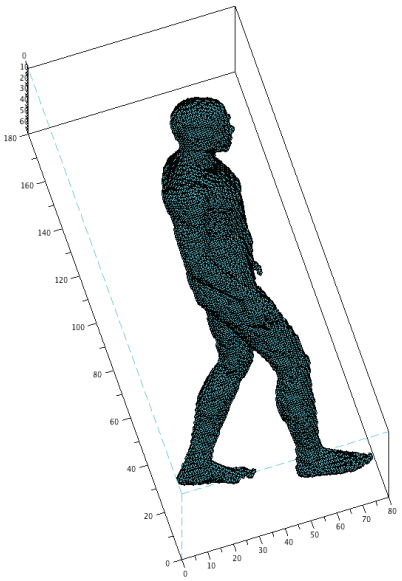

Fig. 3. Example of the generated voxels for walking to be used by FDTD simulations

TABLE I

Average, worst and best received level for Tx-Rx direction combinations for the walking.

Tx-Rx	Avg	Worst	Best
Tx:U-Rx:U	-94.9	-137	-77.9
Tx:U-Rx:V	-99.4	-151	-78.9
Tx:V-Rx:U	-101	-136	-81.8
Tx:V-Rx:V	-95.0	-145	-75.7

the statistical characteristics for each Tx-Rx direction combinations for the walking. The 'Avg' shows the averaged received level through the moving duration, the 'Worst' shows the worst received level, and the 'Best' shows the best received level respectively.

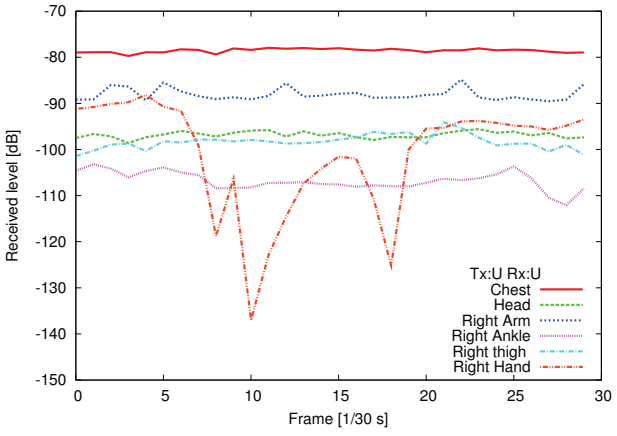

Fig. 4. Temporal received level (walking, Tx$\mathbf{u}$-Rx$\mathbf{u}$)

As shown in table I, Tx:U-Rx:U case shows the best propagation characteristics. However, even in this case, the worst level is -137 dB. It is below -42dB from the average level. To improve this worst level, we propose following simple polarization diversity.

- Two transmitter-receiver combination is used for communication (Combination of four Tx-Rx set U-U, U-V, V-U, and V-V). Totally six cases are considered (U-U and U-V, U-U and V-U, U-U and V-V, U-V and V-U, U-V and V-V, V-U and V-V).
- Received power $r_s[t]$ of time step t is selected according to level comparison of previous time step (between $r_1[t-$

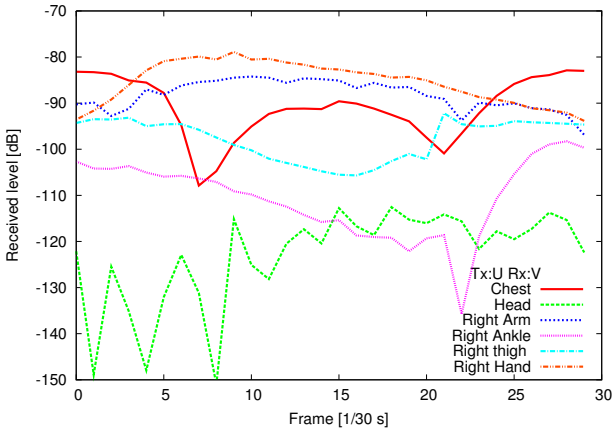

Fig. 5. Temporal received level (walking, Tx**u**-Rx**v**)

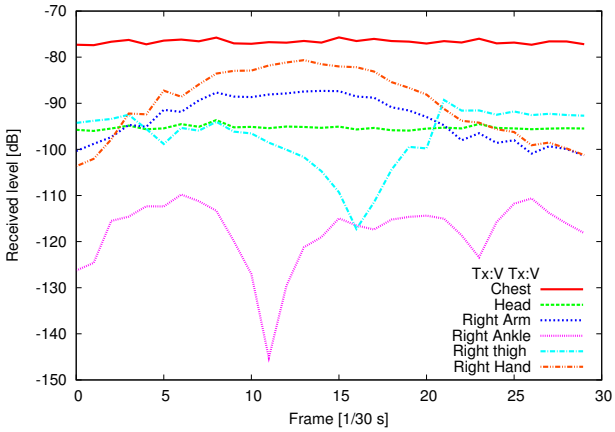

Fig. 6. Temporal received level (walking, Tx**v**-Rx**v**)

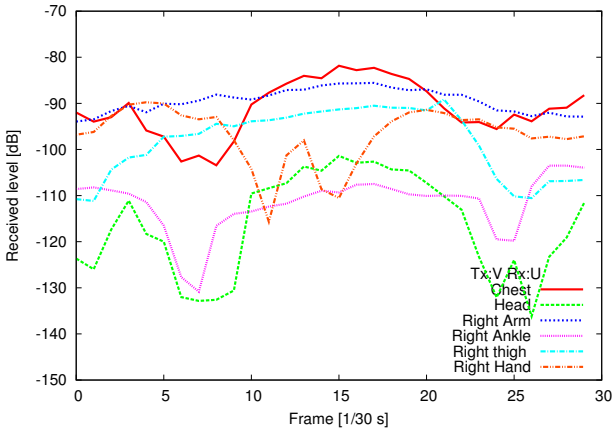

Fig. 7. Temporal received level (walking, Tx**v**-Rx**u**)

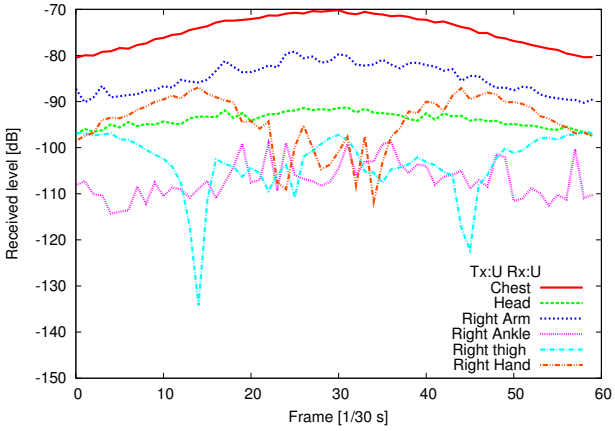

Fig. 8. Temporal received level (Sit/standing, Tx**u**-Rx**u**)

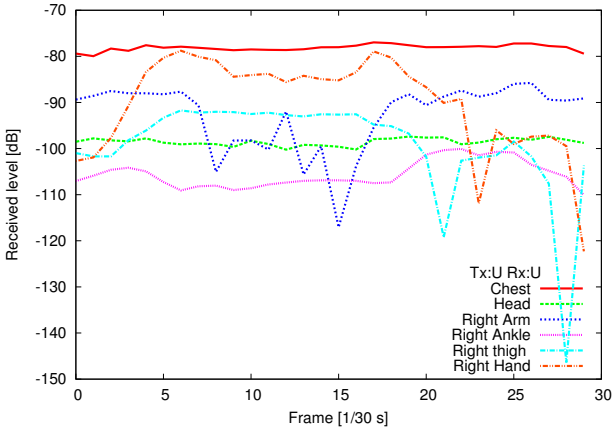

Fig. 9. Temporal received level (Running, Tx**u**-Rx**u**)

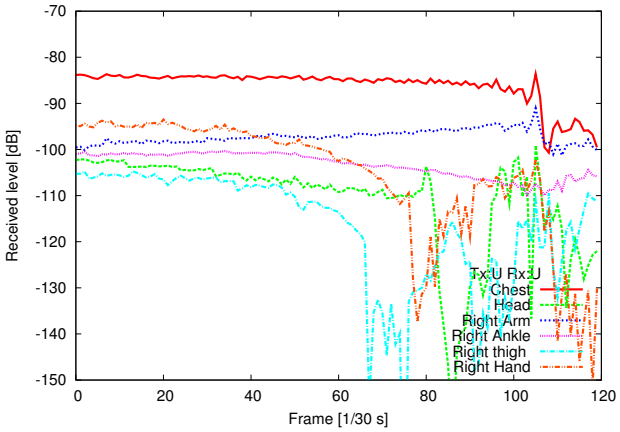

Fig. 10. Temporal received level (Sleeping, Tx**u**-Rx**u**)

TABLE II

AVERAGE, WORST AND BEST RECEIVED LEVEL FOR POLARIZATION DIVERSITY COMBINATIONS FOR THE WALKING.

Combination of Tx-Rx	Avg	Worst	Best
Tx:U-Rx:U and Tx:U-Rx:V	-91.6	-109	-77.9
Tx:U-Rx:U and Tx:V-Rx:U	-93.6	-116	-77.9
Tx:U-Rx:U and Tx:V-Rx:V	-91.8	-112	-75.7
Tx:U-Rx:V and Tx:V-Rx:U	-96.5	-151	-78.9
Tx:U-Rx:V and Tx:V-Rx:V	-92.1	-123	-75.7
Tx:V-Rx:U and Tx:V-Rx:V	-92.6	-124	-75.7

$1]$ and $r_2[t-1]$), where r_1 and r_2 are received level of transmitter-receiver combinations.

Table II concludes the polarization diversity consideration for the walking. According to the table, it seems that the Tx:U-Rx:U and Tx:U-Rx:V case gives best combination. The worst level is improved to -109 dB, the level down from average level is reduced to 17.4 dB.

Figure 13 shows the result of the combination of Tx:U-Rx:U and Tx:U-Rx:V case. As shown in the figure, the received level of the hand is greatly improved. Received level of other positions are also improved. The worst level is above -109 dB for all positions and for all time duration. The worst level is improved by $+28\,\mathrm{dB}$ in comparison with best case of no-polarization-diversity (Tx:U-Rx:U).

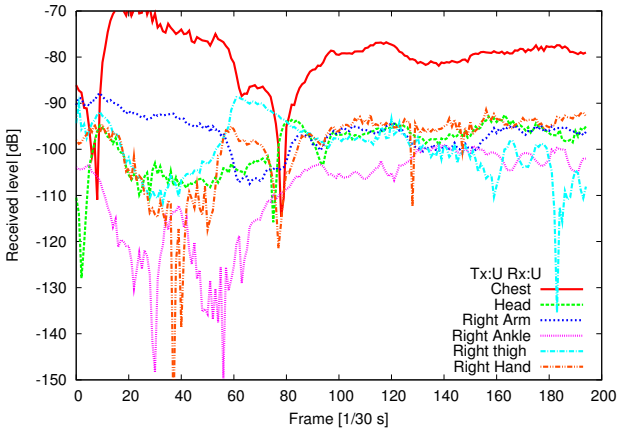

Fig. 11. Temporal received level (Changing cloth, Tx**u**-Rx**u**)

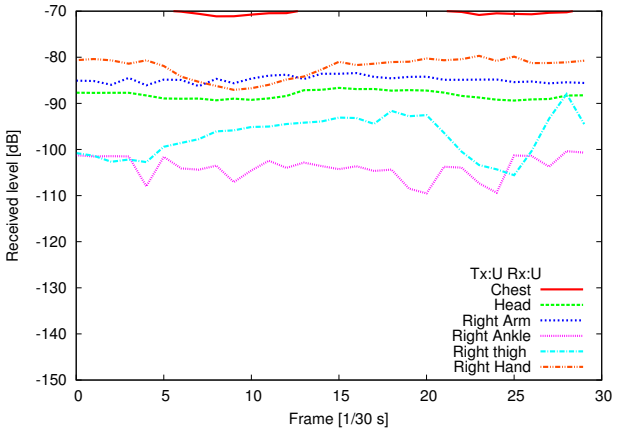

Fig. 12. Temporal received level (Weak walking, Tx**u**-Rx**u**)

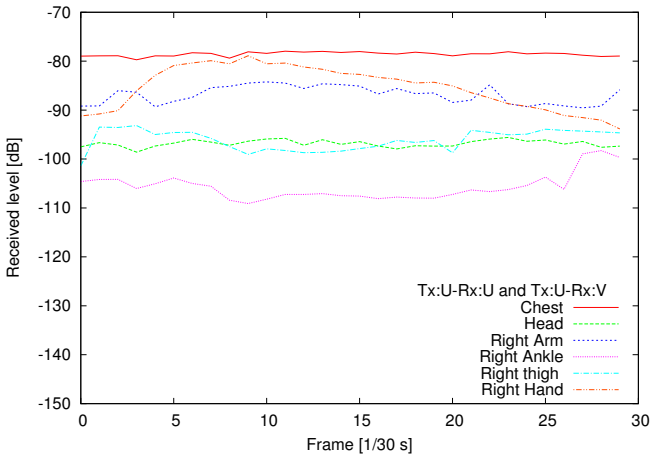

Fig. 13. Polarization diversity result (Tx:U-Rx:U and Tx:U-Rx:V) for the walking.

TABLE III

AVERAGE OF THE WORST DIVERSITY EFFECTS (r_s) FOR TX-RX COMBINATIONS

Combination (Tx-Rx)	Avg (r_s)	r_1	r_2
U-U and U-V**	-123.7	-147.0	-152.8
U-U and V-U	-127.6	-147.0	-149.2
U-U and V-V*	-122.1	-147.0	-152.9
U-V and V-U	-143.2	-153.0	-149.2
U-V and V-V	-136.7	-152.0	-152.9
U-U and V-V	-136.8	-149.0	-152.9

*: Best of the combinations
**: 2nd of the combinations

V. DIVERSITY EFFECTS FOR VARIOUS MOVEMENTS

We have found that the diversity has enough effectiveness for BAN propagation, even if the algorithm was simple selection diversity. Secondary, we tried to see diversity effectiveness for all six movements. Table III shows averages of the worst diversity effects for each Tx-Rx for all six movements. In the Table III, U-U and V-V combination (*) shows the best average receive level, and U-U and U-V combination (**) shows the second best. As we found in the walking motion case, U-U and V-V combination or U-U and U-V combination also shows good diversity effectiveness for all motions.

Table IV shows the temporal and positional average of received level of individual receiving positions for all motions with UU-UV diversity combination. As shown in the table IV, temporal averaged levels are in $10\,\mathrm{dB}$ range for all motions. However, for the sleeping and the cloth changing, the worst received levels are going down below $-140\,\mathrm{dB}$. We think that for these two movements, the human motions are smaller and slower than the other movements. Thus the diversity effectiveness become lower for these movements. We

TABLE IV

DIVERSITY EFFECTIVENESS OF EVERY MOVEMENTS FOR UU-UV DIVERSITY.

	Worst of r_s	Average of temporal average for all positions	Average of worst level for all positions
Walking	-112.0	-93.0	-122.0
Sit/Standing	-122.9	-90.2	-130.0
Running	-110.1	-92.8	-123.0
Weak walking	-109.5	-88.7	-125.0
Sleeping	-146.7	-97.8	-157.9
Cloth changing	-141.3	-94.0	-133.0

should develop BAN communication systems as avoiding this problem by some other propagation diversity techniques or communication protocol.

VI. CONCLUSION

In this report, we performed six human movement simulation by a commercial software (Poser7). We performed FDTD simulations for body area network propagation with one transmitter and six receivers. Received amplitudes were calculated for every time frame of 1/30 s interval. We also demonstrated a polarization diversity effectiveness for dynamic wearable body area network propagation. The followings are left for further study.

- Make a dynamic BAN channel model by using the results.
- Make some correlation of the simulations to measurements to gauge the value of the simulation and methodology by introducing an actual antenna structure into FDTD simulation.
- Communication simulations (e.g. BER) can be performed by using the results. To determine absolute power, measured antenna power is needed [11].
- We may find best antenna direction for individual antenna positions.
- We are going to perform electromagnetic propagation simulation for rest movements. Other frequencies (e.g. 2450 MHz or UWB band) are also to be simulated.
- One more direction ($\mathbf{w} = \mathbf{u} \times \mathbf{v}$), perpendicular to human surface, might be considered for transmitter and receivers.
- Magnetic current source should be considered.

REFERENCES

[1] K. Y. Yazdandoost and K. Sayrafian, "Channel model for body area network (BAN)," IEEE P802.15-08-0033-07-0006, Nov. 2008.

[2] P. S. Hall and Y. Hao, "Antennas and propagation for body centric communications," in *Proc. Europian conf. on antennas and propagation*, Nov. 2006.

[3] Y. I. Nechayev, P. S. Hall, I. Khan, and C. C. Constantinou, "Wireless ahannels and antennas for body-area-networks," in *Proc. Intl. Conf. Wireless on-demand network systems and services (WONS)*, Feb. 2010.

[4] P. S. Hall, Y. Hao, and S. L. Cotton, "Progress in antennas and propagation for body area networks," in *Proc. Intl. Symp. on Signals, Systems and Electronics (ISSE2010)*, Sept. 2010.

[5] A. Fort, J. Ryckaert, C. Desset, P. D. Doncker, P. Wambacq, and L. V. Biesen, "Ultra-wideband channel model for communication around the human body," *IEEE journal on selected areas in comm.*, vol. 24, pp. 927–933, 2006.

[6] A. Fort, C. Desset, P. Wambacq, and L. B. nV., "Indoor body-area channel model for narrowband communications," *IET Microw. Antennas Propagation*, vol. 1, pp. 1197–1203, 2007.

[7] T. Zasowski, G. Meyer, F. Althaus, and A. Wittneben, "Propagation effects in uwb body area networks," in *IEEE Intl. conf. on Ultra-wideband*, Sept. 2005.

[8] H. Sawada, T. Aoyagi, J. Takada, K. Y. Yazdandoost, and R. Kohno, "Channel model for wireless body area network," in *Proc. 2nd Intl. Symp. on Med. Info. and Comm. Tech. (ISMICT)*, Oulu, Finland, Dec. 2007.

[9] K. Takizawa, T. Aoyagi, K. Hamaguchi, and R. Kohno, "Channel models for wireless body area networks," in *Proc. 30th Annual International IEEE EMBS Conference*, Vancouver, British Columbia, Canada, Aug. 2008, pp. 1549–1552.

[10] N. Katayama, K. Takizawa, T. Aoyagi, J. Takada, H.-B. Li, and R. Kohno, "Channel model on various frequency bands for wearable body area network," *IEICE Trans. comm.*, vol. E92-B, no. 2, pp. 418–424, Feb. 2009.

[11] T. Aoyagi, J. Takada, K. Takizawa, H. Sawada, N. Katayama, K. Y. Yazdandoost, T. Kobayashi, H.-B. Li, and R. Kohno, "Channel model for wearable and implantable WBANs," IEEE 802.15-08-0416-04-0006, Nov. 2008.

[12] J. Hagedorn, J. Terrill, W. Tang, K. Sayrafian, K. Y. Yazdandoost, and R. Kohno, "A statistical path loss model for MICS," IEEE 802.15-08-0519-01-0006, Sept. 2008.

[13] S. L. Cotton and W. G. Scanlon, "Characterization of the on-body channel in an outdoor environment at 2.45 ghz," in *European conf. on antennas propagation*, 2009, pp. 722–725.

[14] S. L. Cotton, G. A. Conway, and W. G. Scanlon, "A time-domain approach to the analysis and modeling of on-body propagation characteristics using synchronized measurements at 2.45 ghz," *IEEE trans. on antennas and propagation*, vol. 57, no. 4, pp. 943–955, 2009.

[15] M. Maman, F. Dehmas, R. D'Errico, and L. Ouvry, "Evaluation a tdma mac for body area networks using a space-time dependent channel model," in *Proc. IEEE symp. on personal indoor and mobile radio communications*, Sept. 2009.

[16] M. Kim and J. Takada, "Statistical model for 4.5 GHz narrowband on-body propagaton channel with specific actions," *IEEE Antennas Wireless Propagat. Lett.*, vol. 8, pp. 1250–1254, 2009.

[17] B. Zhen, M. Kim, J. Takada, and R. Kohno, "Characterization and modeling of dynamic on-body propagation," in *Proc. 3rd Intl. Conf. Pervasive Computing Technologies for Healthcare*, London, UK, Apr. 2009.

[18] B. Zhen, M. Kim, J. Takada, and R. Kohno, "Characterization and modeling of dynamic on-body propagation at 4.5 GHz," *IEEE Antennas Wireless Propagat. Lett.*, vol. 8, pp. 1263–1267, 2009.

[19] M. Gallo, P. S. Hall, Y. I. Nechayev, and M. Bozzetti, "Use of animation software in simulation of on-body communications channels at 2.45 GHz," *IEEE Antennas Wireless Propagat. Lett.*, vol. 7, pp. 321–324, 2008.

[20] T. Aoyagi, K. Hamaguchi, and R. Kohno, "Composition of dynamic wearable body area network propagation channel by using numerical simulations," in *Proc. 4th Intl. Symp. on Med. Info. and Comm. Tech. (ISMICT)*, Taipei, Mar. 2010.

[21] S. Gabriel, R. W. Lau, and C. Gabriel, "The dielectric properties of biological tissues: III. Parametric models for the dielectric spectrum of tissues," *Phys. Med. Biol.*, vol. 41, pp. 2271–2293, 1996.

[22] Body tissue dielectric parameters tool. FCC Radio Frequency Safety. [Online]. Available: http://www.fcc.gov/oet/rfsafety/dielectric.html